

Sol-Gel Synthesis, Structural and Optical Properties of Cerium-Doped Strontium Aluminates, $\text{Sr}_3\text{Al}_2\text{O}_6$ and $\text{SrAl}_{12}\text{O}_{19}$

Martynas MISEVIČIUS^{1*}, Jens-Erik JØRGENSEN², Aivaras KAREIVA¹

¹ Department of General and Inorganic Chemistry, Vilnius University, Naugarduko 24, LT-03225 Vilnius, Lithuania

² Department of Chemistry, Aarhus University, Langelangsgade 140, 8000 Aarhus C, Denmark

crossref <http://dx.doi.org/10.5755/j01.ms.19.4.2670>

Received 23 October 2012; accepted 08 July 2013

In this study, an aqueous sol-gel synthesis method was applied for the preparation of strontium aluminate ($\text{Sr}_3\text{Al}_2\text{O}_6$ and $\text{SrAl}_{12}\text{O}_{19}$) ceramics. The structural properties of these compounds were investigated by X-ray powder diffraction analysis. The obtained data were analysed employing Rietveld method. Optical properties of sol-gel derived cerium-doped strontium aluminates showed emission maxima at 480 nm and 317 nm for $\text{Sr}_3\text{Al}_2\text{O}_6:\text{Ce}$ and $\text{SrAl}_{12}\text{O}_{19}:\text{Ce}$, respectively.

Keywords: strontium aluminates, sol-gel synthesis, X-ray diffraction, Rietveld refinement, cerium doping, luminescence.

1. INTRODUCTION

In $\text{SrO-Al}_2\text{O}_3$ system, there are four stable double oxides, namely $\text{Sr}_3\text{Al}_2\text{O}_6$, SrAl_2O_4 , SrAl_4O_7 and $\text{SrAl}_{12}\text{O}_{19}$, and other strontium aluminate phases, such as $\text{Sr}_4\text{Al}_2\text{O}_7$, $\text{Sr}_4\text{Al}_{14}\text{O}_{25}$, $\text{Sr}_{12}\text{Al}_{14}\text{O}_{33}$ and $\text{Sr}_{10}\text{Al}_6\text{O}_{19}$, as described in the literature [1]. The most publications on strontium aluminate phases are related with the strong green emission (~530 nm) of Eu^{2+} in stoichiometric SrAl_2O_4 with monoclinic trydimite structure [2, 3]. It was reported that $\text{SrAl}_2\text{O}_4:\text{Eu}^{2+},\text{Dy}^{3+},\text{B}^{3+}$ has greatly enhanced phosphorescence properties compared not only with $\text{SrAl}_2\text{O}_4:\text{Eu}^{2+}$ but also with $\text{ZnS}:\text{Cu}^+,\text{Co}^{2+}$. In addition to higher chemical stability, the intensity and the duration of the phosphorescence of $\text{SrAl}_2\text{O}_4:\text{Eu}^{2+},\text{Dy}^{3+},\text{B}^{3+}$ make it possible to observe a continuous light emission for 10 h, hence greatly renewing interests in the phosphorescence phenomenon [4].

The $\text{Sr}_3\text{Al}_2\text{O}_6$ phase has a cubic structure with space group $Pa-3$ (No. 205) [5]. It can be obtained using solid-state reaction and it is possible to shorten processing times compared to conventional processes by using mechanically activated SrCO_3 as a starting material [6]. Investigation of europium and dysprosium doped $\text{Sr}_3\text{Al}_2\text{O}_6$ revealed, that different oxidation state of Eu gives different photoluminescence, moreover only Eu^{2+} showed excellent afterglow, compared with almost none in case of Eu^{3+} [7]. Li et al. synthesized $\text{Sr}_3\text{Al}_2\text{O}_6:\text{Ce}^{3+}$ phosphor using a solid state synthesis method. The measured emission spectrum showed a broad band, which can be resolved into two emission bands peaking at 455 nm and 487 nm [8].

The $\text{SrAl}_{12}\text{O}_{19}$ phase has a hexagonal structure with space group $P6_3/mmc$ (No. 194) [9]. Polycrystalline $\text{SrAl}_{12}\text{O}_{19}:\text{Mn}$ is known as a green-emitting phosphor for plasma display panels. Praseodymium or neodymium doped $\text{SrAl}_{12}\text{O}_{19}$ crystals show good laser properties [10]. It is reported that $\text{Sr}_{0.95}\text{Ce}_{0.05}\text{Mg}_{0.05}\text{Al}_{11.95}\text{O}_{19}$ has the

emission maximum at 305 nm and yields quantum efficiency of 70 % [11].

Recently we presented results of a systematic study of aqueous sol-gel synthetic approach to pure and Ce-doped strontium aluminates SrAl_2O_4 , $\text{Sr}_3\text{Al}_2\text{O}_6$, $\text{Sr}_4\text{Al}_4\text{O}_{10}$, $\text{SrAl}_{12}\text{O}_{19}$ and $\text{Sr}_4\text{Al}_{14}\text{O}_{25}$ using glycolate intermediates [12]. However, the impurity phases (SrCO_3 , SrAl_2O_4 , Al_2O_3 and unknown) were the dominating components during the synthesis of $\text{SrAl}_{12}\text{O}_{19}$ ceramics in the temperature range of 700 °C–1000 °C. Therefore, in this study we continue to optimize parameters of sol-gel processing to obtain monophasic undoped and Ce-doped $\text{Sr}_3\text{Al}_2\text{O}_6$ and $\text{SrAl}_{12}\text{O}_{19}$ compounds, to refine their crystal structures and investigate luminescent properties of obtained cerium-doped samples.

2. EXPERIMENTAL

Sol-gel synthesis method was employed in order to obtain single phase strontium aluminates $\text{Sr}_3\text{Al}_2\text{O}_6$, $\text{SrAl}_{12}\text{O}_{19}$, $\text{Sr}_3\text{Al}_2\text{O}_6:\text{Ce}$ and $\text{SrAl}_{12}\text{O}_{19}:\text{Ce}$. Stoichiometric amounts of $\text{Al}(\text{NO}_3)_3 \cdot 9\text{H}_2\text{O}$ ($\geq 98\%$ Aldrich), $\text{Sr}(\text{NO}_3)_2$ ($\geq 99\%$ Aldrich) and $\text{Ce}(\text{NO}_3)_6 \cdot 6\text{H}_2\text{O}$ ($\geq 99\%$ Merck) were dissolved in 0.2 M acetic acid solution and 2 mL of 1,2-ethanediol was added as a complexing agent. After stirring for 1 h, the obtained solutions were evaporated to form gels, which then were preheated for 8 h at 800 °C. Obtained white powders were thoroughly ground in agate mortar and further sintered at 900 °C–1600 °C.

Powder X-ray diffraction (XRD) analysis has been carried out employing Rigaku Smartlab diffractometer working in parallel beam ($\theta/2\theta$) geometry, using 2.5° Soller slits and CuK_α radiation. Samples were spun at 30 rpm. Measurements were taken at step of 0.02° and at speed of 4 s/step. XRD analysis of cerium doped samples has been carried out employing Rigaku MiniFlex II diffractometer working in Bragg-Brentano ($\theta/2\theta$) geometry. The data were collected at a step of 0.01° and at speed of 0.06 s/step using CuK_α radiation. Rietveld refinement was performed on the data using the software *FullProf* [13]. The residuals were calculated as following:

*Corresponding author. Tel: +370 682 65807, fax: +370 682 65807.
E-mail address: martynas.misevicius@chf.vu.lt (M. Misevičius)

$$R_{wp} = 100 \left[\frac{\sum_{i=1,n} w_i |y_i - y_{c,i}|^2}{\sum_{i=1,n} w_i y_i^2} \right]^{1/2}; \quad (1)$$

$$R_{exp} = 100 \left[\frac{n-p}{\sum_i w_i y_i^2} \right]^{1/2}; \quad (2)$$

$$\chi^2 = \left[\frac{R_{wp}}{R_{exp}} \right]^2,$$

where R_{wp} is the weighted profile factor, R_{exp} – expected weighted profile factor, y_i - the observed intensity of the i th data pint, $y_{c,i}$ – the calculated intensity of the i th data point, w_i – the weight of the i th data point, n is the total number of data points, p is the number of refined parameters [13, 14].

UV-Vis reflectance spectra were recorded in the range of 2600 nm–220 nm at step of 2 nm on Shimadzu UV-3600 spectrophotometer equipped with integration sphere. BaSO₄ was used as a reflectance standard. Excitation and emission spectra were recorded on PerkinElmer LS-55 fluorescence spectrometer.

3. RESULTS AND DISCUSSION

3.1. Sr₃Al₂O₆

The strontium aluminate samples of Sr₃Al₂O₆ and Sr₃Al₂O₆:Ce were prepared according to the sol-gel

method developed in our previous study [12]. Undoped Sr₃Al₂O₆ sample was characterized by powder X-ray diffraction analysis and obtained data were analyzed employing Rietveld refinement method [15, 16]. The original crystallographic data of Sr₃Al₂O₆ (ICSD#71860) were used as a starting model. Rietveld analysis results are shown in Figure 1. During structure refinement it was noticed, that not all diffraction peaks observed in the XRD pattern are covered. Therefore, two additional phases, such as SrAl₂O₄ (ICSD#160296) and SrAl₄O₇ (ICSD#2817) were added to the starting model. The refinement smoothly converged to the structure close to the starting model based on X-ray powder diffraction data. Therefore, it was determined that the phase of interest (Sr₃Al₂O₆) makes only about 60 % of the specimen. This was impossible to determine without Rietveld refinement, because cubic Sr₃Al₂O₆ structure gives very intensive reflection at $2\theta = 31.9^\circ$ and it becomes difficult to separate low intensity peaks from background noise.

Figure 2 shows UV-Vis reflection and photoluminescence measurements data of undoped (Sr₃Al₂O₆) and Ce³⁺ doped strontium aluminate (Sr₃Al₂O₆:Ce) samples having different concentration of cerium. There is clearly visible difference in the optical properties of doped and undoped samples. From the reflection spectra we can see that cerium ions increase absorption in the region of around 300 nm. Excitation spectra of sol-gel derived strontium aluminates shows maximum at 268 nm. As seen, the intensity of excitation bands increases with increasing concentration of cerium.

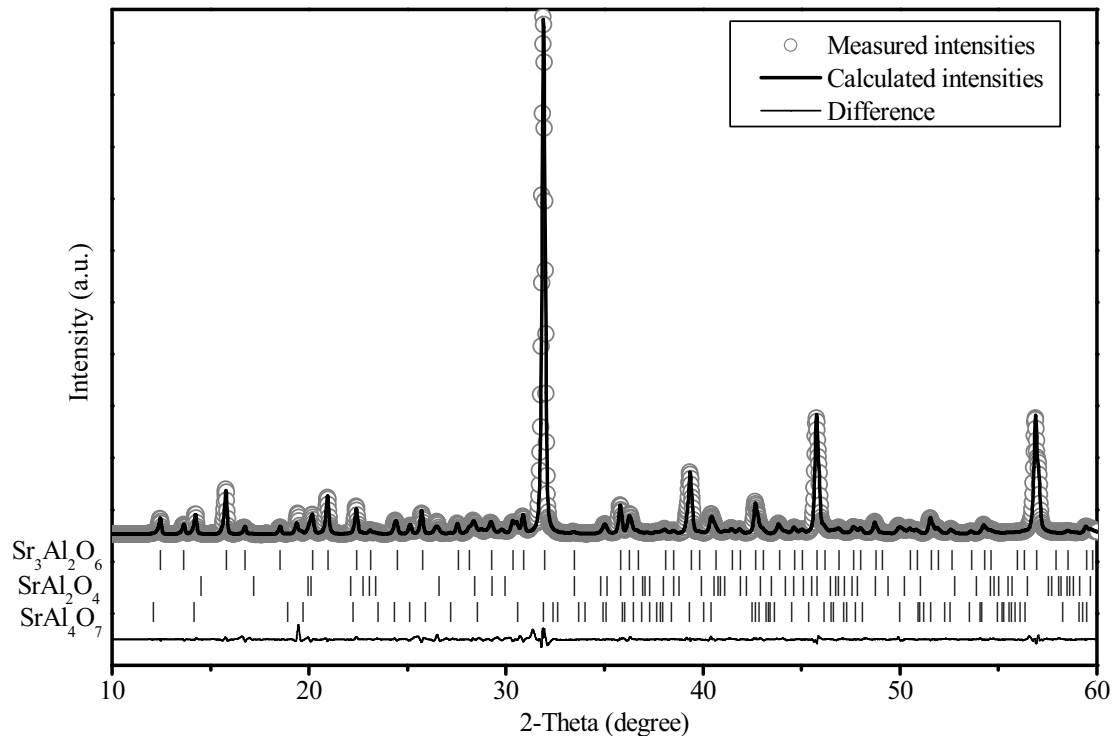


Fig. 1. The observed (circles) and calculated (solid line) powder XRD patterns of Sr₃Al₂O₆ sample after Rietveld refinement. The vertical bars located just below the background level indicate calculated positions of Bragg peaks for $\lambda K\alpha_1$. The curve in the bottom part of the plot represents the difference between observed and calculated intensities. Goodness of fit indicators: $\chi^2 = 0.40$; $R_{wp} = 10.81\%$

The measured emission spectra show a broad emission band peaked at 480 nm. Again, the measured emission intensities increase with increasing Ce^{3+} concentration in the series of samples up to 3 % of cerium. Obtained results are in a good agreement with the study of $\text{Sr}_3\text{Al}_2\text{O}_6:\text{Ce}$ compounds, synthesized using solid state reaction [8].

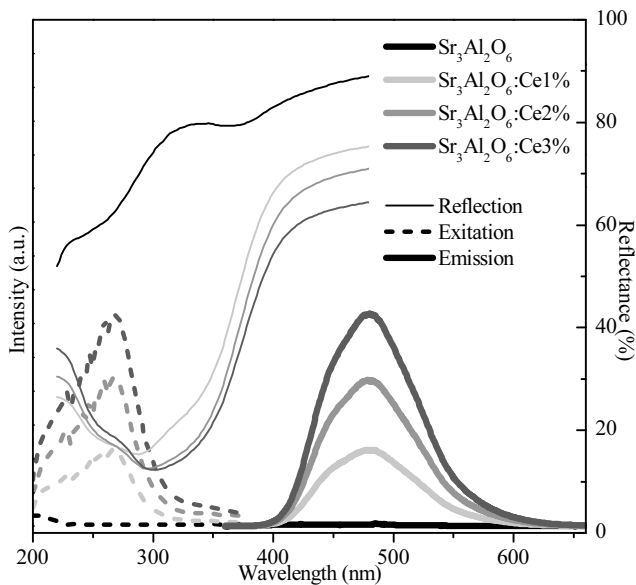


Fig. 2. Reflection, excitation and emission spectra of $\text{Sr}_3\text{Al}_2\text{O}_6$ and $\text{Sr}_3\text{Al}_2\text{O}_6:\text{Ce}$ samples

3.2. $\text{SrAl}_{12}\text{O}_{19}$

The formation of $\text{SrAl}_{12}\text{O}_{19}$ aluminate at elevated temperatures was previously found to be very problematic

[12]. In order to determine phase formation conditions of $\text{SrAl}_{12}\text{O}_{19}$ aluminate, a series of samples prepared using aqueous sol-gel method were annealed at high temperatures ranging from 1200 °C to 1600 °C. The XRD patterns of calcined at different temperatures samples are shown in Figure 3.

As seen from Fig. 3, that the samples annealed at 1500 °C–1600 °C are single phase $\text{SrAl}_{12}\text{O}_{19}$ compounds. The synthesis products obtained in the temperature range of 1200 °C–1400 °C contained impurity phases, such as SrAl_2O_4 and Al_2O_3 . To prove the formation of monophasic $\text{SrAl}_{12}\text{O}_{19}$ at 1500 °C, this sample was analyzed more precisely. The precise X-ray diffraction data were collected and refined using Rietveld technique. The original crystallographic data of $\text{SrAl}_{12}\text{O}_{19}$ (ICSD#43155) were used as a starting model. Results of the Rietveld refinement are shown in Figure 4.

During refinement it was noticed, that not all diffraction peaks presented in the XRD pattern are covered. Therefore, crystallographic data of SrAl_2O_4 (ICSD#160296) were added to the starting model. The refinement smoothly converged to the structure close to the starting model based on X-ray powder diffraction data. It was determined that second phase makes up only traces (less than 1 %). Thus, the obtained $\text{SrAl}_{12}\text{O}_{19}$ sample using sol-gel technique is pure enough.

Figure 5 shows UV-Vis reflection and photoluminescence measurements data of undoped ($\text{SrAl}_{12}\text{O}_{19}$) and Ce^{3+} doped strontium aluminate ($\text{SrAl}_{12}\text{O}_{19}:\text{Ce}$) samples having different concentration of cerium. In the reflection spectra it is visible that Ce^{3+} ions originate absorption peaks at around ~226 nm, ~244 nm and ~274 nm. Excitation and

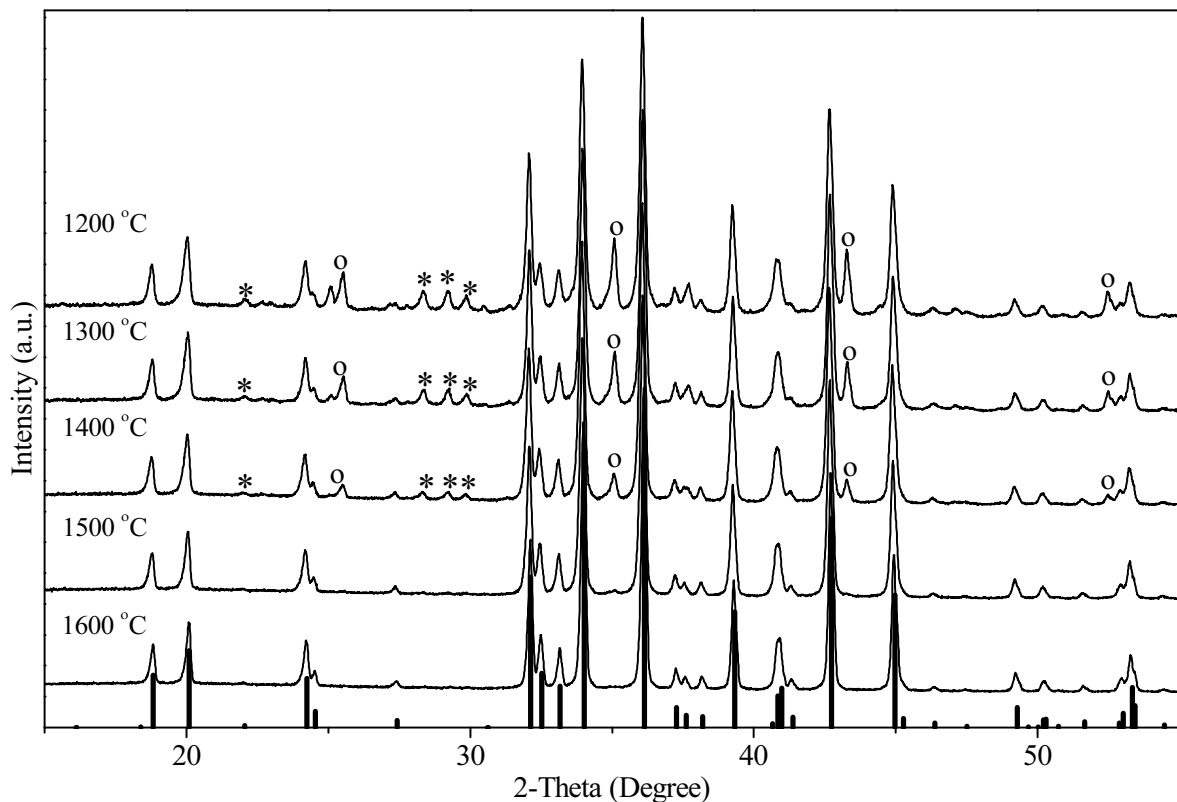


Fig. 3. XRD patterns of $\text{SrAl}_{12}\text{O}_{19}$ samples annealed at different temperatures. Solid lines at the bottom of figure represent $\text{SrAl}_{12}\text{O}_{19}$ (PDF#00-080-1195). The side phases are marked: * – SrAl_2O_4 (PDF#00-046-1212) and \circ – Al_2O_3 (PDF#00-088-0826)

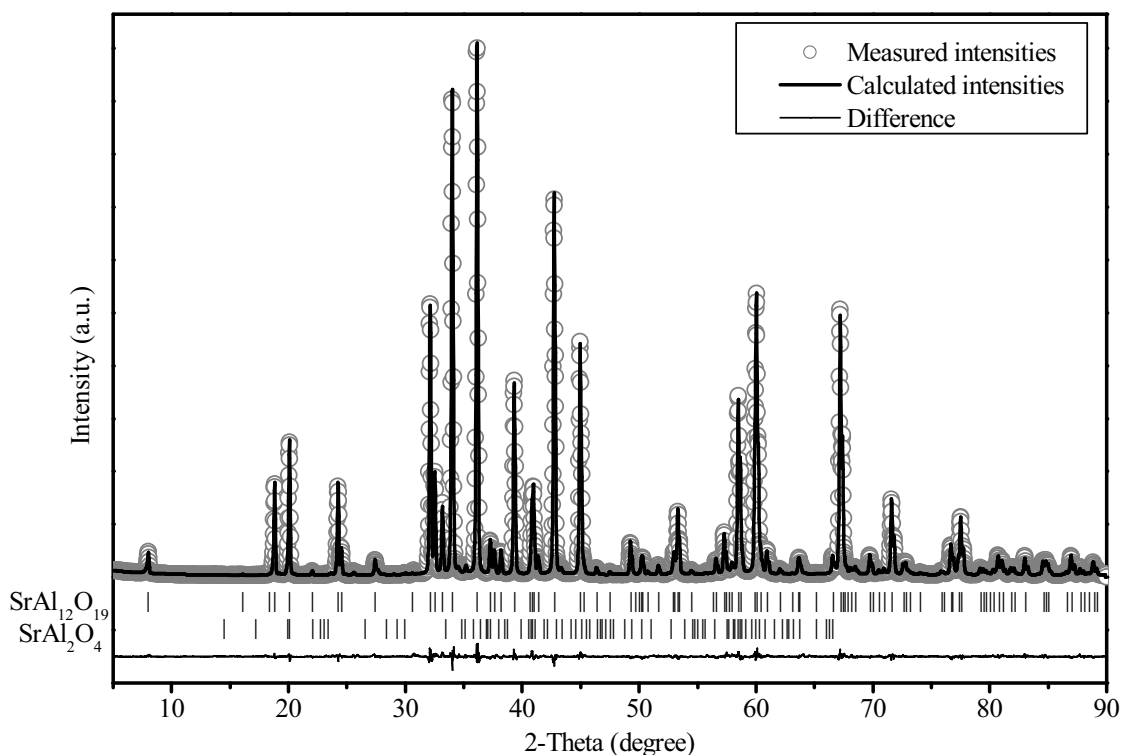


Fig. 4. The observed (circles) and calculated (solid line) powder XRD patterns of $\text{SrAl}_{12}\text{O}_{19}$ sample after Rietveld refinement. The vertical bars located just below the background level indicate calculated positions of Bragg peaks for $\lambda K\alpha_1$. The curve in the bottom part of the plot represents the difference between observed and calculated intensities. Goodness of fit indicators: $\chi^2 = 0.30$; $R_{wp} = 5.58\%$

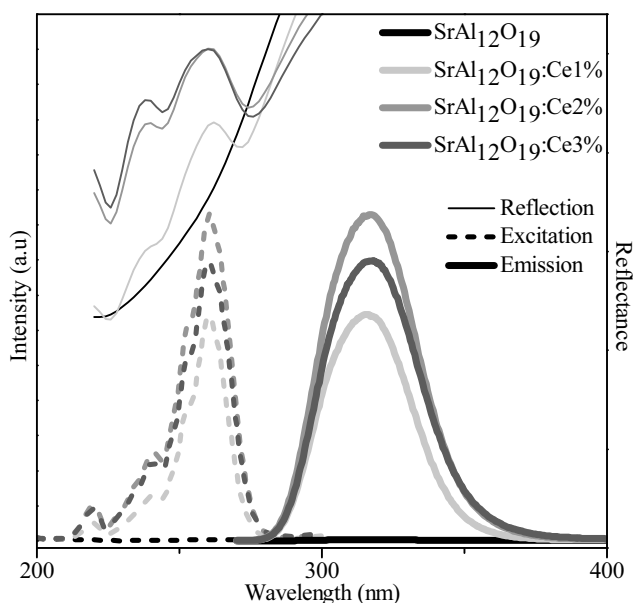


Fig. 5. Reflection, excitation and emission spectra of $\text{SrAl}_{12}\text{O}_{19}$ and $\text{SrAl}_{12}\text{O}_{19}:\text{Ce}$ samples

emission maxima of $\text{SrAl}_{12}\text{O}_{19}:\text{Ce}$ samples are clearly visible at 260 nm and 317 nm, respectively. These results are similar to the luminescence measurements of $\text{Sr}_{0.95}\text{Ce}_{0.05}\text{Mg}_{0.05}\text{Al}_{11.95}\text{O}_{19}$ [11]. Interestingly, the photoluminescence spectra of $\text{SrAl}_{12}\text{O}_{19}:\text{Ce}$ samples shows, that the highest intensity is when cerium concentration reaches 2%. With increasing concentration of cerium the decreasing of the emission intensity is observed due to the concentration quenching [17].

The obtained results in this study clearly demonstrate the influence of matrix on the luminescent properties of cerium. As was observed, the $\text{Sr}_3\text{Al}_2\text{O}_6:\text{Ce}$ samples show a broad emission band at ~ 480 nm without concentration quenching effect up to 3% of cerium. However, the emission maximum observed for $\text{SrAl}_{12}\text{O}_{19}:\text{Ce}$ samples has shifted dramatically to the lower wavelength region (317 nm). Moreover, the concentration quenching was observed at 3% of cerium.

4. CONCLUSIONS

Aqueous sol-gel method was used for the synthesis of undoped and cerium-doped $\text{Sr}_3\text{Al}_2\text{O}_6$ and $\text{SrAl}_{12}\text{O}_{19}$ strontium aluminates. The single phase $\text{SrAl}_{12}\text{O}_{19}$ was obtained after calcination of precursor gels at 1500°C . The luminescent spectra revealed that emission maxima for $\text{Sr}_3\text{Al}_2\text{O}_6:\text{Ce}$ and $\text{SrAl}_{12}\text{O}_{19}:\text{Ce}$ are located at 480 nm and 317 nm, respectively, indicating strong matrix effect on the luminescent properties of cerium.

Acknowledgments

The study was funded from the European Community's social foundation under Grant Agreement No. VP1-3.1-ŠMM-08-K-01-004/KS-120000-1756"

REFERENCES

1. Douy, A., Capron, M. Crystallisation of Spray-dried Amorphous Precursors in the $\text{SrO}-\text{Al}_2\text{O}_3$ System: a DSC Study *Journal of the European Ceramic Society* 23 (12) 2003: pp. 2075–2081.
[http://dx.doi.org/10.1016/S0955-2219\(03\)00015-3](http://dx.doi.org/10.1016/S0955-2219(03)00015-3)

2. **Haranath, D., Virendra, S., Harish, C., Pooja, S.** Tuning of Emission Colours in Strontium Aluminate Long Persisting Phosphor *Journal of Physics D: Applied Physics* 36 (18) 2003: pp. 2244–2248.
3. **Avdeev, M., Yakovlev, S., Yaremchenko, A. A., Kharton, V. V.** Transitions between P₂₁, P₆₃ and P₆₃₂₂ Modifications of SrAl₂O₄ by In Situ High-temperature X-ray and Neutron Diffraction *Journal of Solid State Chemistry* 180 (12) 2007: pp. 3535–3544.
4. **Clabau, F., Rocquefelte, X., Jobic, S., Deniard, P., Whangbo, M. H., Garcia, A., Le Mercier, T.** Mechanism of Phosphorescence Appropriate for the Long-Lasting Phosphors Eu²⁺-Doped SrAl₂O₄ with Codopants Dy³⁺ and B³⁺ *Chemistry of Materials* 17 (15) 2005: pp. 3904–3912. <http://dx.doi.org/10.1021/cm050763r>
5. **Chakoumakos, B. C., Lager, G. A., Fernandez-Baca, J. A.** ChemInform Abstract: A Refinement of the Structures of Sr₃Al₂O₆ and the Hydrogarnet Sr₃Al₂(O₄D₄)₃ by Rietveld Analysis of Neutron Powder Diffraction Data *ChemInform* 23 (22) 1992: pp. 414–419.
6. **Garcés, R. S., Torres, J. T., Valdés, A. F.** Synthesis of SrAl₂O₄ and Sr₃Al₂O₆ at High Temperature, Starting from Mechanically Activated SrCO₃ and Al₂O₃ in Blends of 3:1 Molar Ratio *Ceramics International* 38 (2) 2012: pp. 889–894. <http://dx.doi.org/10.1016/j.ceramint.2011.08.021>
7. **Chang, C., Li, W., Huang, X., Wang, Z., Chen, X., Qian, X., Guo, R., Ding, Y., Mao, D.** Photoluminescence and Afterglow Behavior of Eu²⁺, Dy³⁺ and Eu³⁺, Dy³⁺ in Sr₃Al₂O₆ Matrix *Journal of Luminescence* 130 (3) 2010: pp. 347–350. <http://dx.doi.org/10.1016/j.jlumin.2009.09.016>
8. **Li, G., Lai, Y., Cui, T., Yu, H., Liu, D., Gan, S.** Luminescence Properties and Charge Compensation of Sr₃Al₂O₆ Doped with Ce³⁺ and Alkali Metal Ions *Materials Chemistry and Physics* 124 (2–3) 2010: pp. 1094–1099.
9. **Lindop, A. J., Matthews, C., Goodwin, D.W.** The Refined Structure of SrO₆Al₂O₃ *Acta Crystallographica Section B* 31 (12) 1975: pp. 2940–2941. <http://dx.doi.org/10.1107/S0567740875009351>
10. **Rodnyi, P. A., Dorenbos, P., Stryganyuk, G. B., Voloshinovskii, A. S., Potapov, A. S., Eijk, C. W. E. V.** Emission of Pr³⁺ in SrAl₁₂O₁₉ under Vacuum Ultraviolet Synchrotron Excitation *Journal of Physics: Condensed Matter*. 15 (4) 2003: pp. 719–729. <http://dx.doi.org/10.1088/0953-8984/15/4/311>
11. **Verstegen, J. M. P. J.** A Survey of a Group of Phosphors, Based on Hexagonal Aluminate and Gallate Host Lattices *Journal of The Electrochemical Society* 121 (12) 1974: pp. 1623–1627.
12. **Misevicius, M., Scit, O., Grigoraviciute-Puroniene, I., Degutis, G., Bogdanoviciene, I., Kareiva, A.** Sol-gel Synthesis and Investigation of Un-doped and Ce-doped Strontium Aluminates *Ceramics International* 38 (7) 2012: pp. 5915–5924.
13. **Rodríguez-Carvajal, J.** An Introduction to the Program FullProf. Saclay, 2001: 139 p.
14. **Pecharsky, V. K., Zavalij, P. Y.** Fundamentals of Powder Diffraction and Structural Characterization of Materials. 2nd ed. Springer, New York, 2009: 744 p.
15. **Rietveld, H.** Line Profiles of Neutron Powder-diffraction Peaks for Structure Refinement *Acta Crystallographica* 22 (1) 1967: pp. 151–152.
16. **Rietveld, H.** A Profile Refinement Method for Nuclear and Magnetic Structures *Journal of Applied Crystallography* 2 (2) 1969: pp. 65–71.
17. **Kareiva, A.** Aqueous Sol-Gel Synthesis Methods for the Preparation of Garnet Crystal Structure Compounds *Materials Science (Medžiagotyra)* 17 (4) 2011: pp. 427–436.